Bacteriophage genomes encode both broad and specific counter-defense repertoires to overcome bacterial defense systems

Costa, Ana Rita; van den Berg, Daan F.; Esser, Jelger Q.; van den Bossche, Halewijn; Pozhydaieva, Nadiia; Kalogeropoulos, Konstantinos; Brouns, Stan J.J.

DOI
10.1016/j.chom.2025.06.010

Publication date
2025

Document Version
Final published version

Published in
Cell Host and Microbe

Article

Cell Host & Microbe

Bacteriophage genomes encode both broad and specific counter-defense repertoires to overcome bacterial defense systems

Graphical abstract

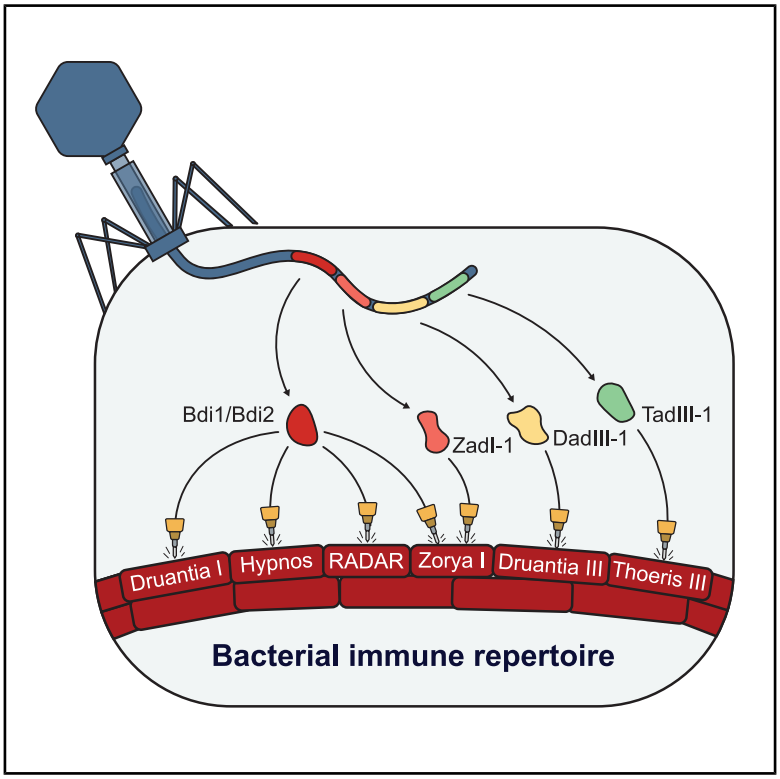

Authors

Ana Rita Costa, Daan F. van den Berg, Jelger Q. Esser, Halewijn van den Bossche, Nadiia Pozhydaieva, Konstantinos Kalogeropoulos, Stan J.J. Brouns

Correspondence

stanbrouns@gmail.com

In brief

Costa, van den Berg, Esser, et al. identify two broad and three specific anti-defense genes by examining variable regions of *Pseudomonas* phage genomes. These inhibitors neutralize diverse bacterial immune systems, highlighting how phages evolve both broad and specific strategies to overcome the host defense repertoire.

Highlights

- Variable regions of phage genomes encode anti-defense genes
- ZadI-1, DadIII-1, and TadIII-1 inhibit specific defense systems
- Bdi1 and Bdi2 neutralize a broad range of defense systems
- Broad defense inhibitors are encoded by phages infecting diverse bacterial clades

Costa et al., 2025, Cell Host & Microbe *33*, 1161–1172
July 9, 2025
https://doi.org/10.1016/j.chom.2025.06.010

CellPress

Cell Host & Microbe

CellPress

Article

Bacteriophage genomes encode both broad and specific counter-defense repertoires to overcome bacterial defense systems

Ana Rita Costa,[1,2,4] Daan F. van den Berg,[1,2,4] Jelger Q. Esser,[1,2,4] Halewijn van den Bossche,[1,2] Nadiia Pozhydaieva,[1,2] Konstantinos Kalogeropoulos,[1,2,3] and Stan J.J. Brouns[1,2,5,*]

[1]Department of Bionanoscience, Delft University of Technology, 2629 HZ Delft, the Netherlands
[2]Kavli Institute of Nanoscience, Delft, the Netherlands
[3]Department of Biotechnology and Biomedicine, Technical University of Denmark, 2800 Kgs Lyngby, Denmark
[4]These authors contributed equally
[5]Lead contact
*Correspondence: stanbrouns@gmail.com
https://doi.org/10.1016/j.chom.2025.06.010

SUMMARY

The evolutionary arms race between bacteria and bacteriophages drives rapid evolution of bacterial defense mechanisms with scattered distribution across genomes. We hypothesized that this variability in bacterial defense systems leads to equally variable counter-defense repertoires in phage genomes. Examining the variable regions in *Pseudomonas* model phages of the *Pbunavirus* genus revealed five anti-defense genes, including one inhibiting Druantia type III named DadIII-1, another targeting Thoeris type III named TadIII-1, one inhibiting Zorya type I named ZadI-1, and two related broad defense inhibitors named Bdi1 and Bdi2 targeting four defenses. A typical *Pbunavirus* encodes up to five known anti-defense genes, some inhibiting four unrelated defense systems with distinct nucleic-acid-targeting mechanisms. Structural homologs of broad-acting Bdi1 and Bdi2 are encoded across diverse phage taxa infecting multiple bacterial hosts. These findings show that phages face a variety of bacterial defenses, driving them to evolve both specific and general strategies to overcome these barriers.

INTRODUCTION

Prokaryotes have evolved an extensive array of defense mechanisms to protect themselves from bacteriophage predation.[1,2] In response, phages have developed countermeasures to overcome these defenses, including mutations that enable them to escape recognition and anti-defense genes that disrupt phage defense systems.[3–5] Well-known examples of the latter include anti-restriction and anti-CRISPR proteins, which disable restriction-modification and CRISPR-Cas systems, respectively.[6–8] With the increasing discovery of phage defense systems,[2,9–13] novel anti-defense genes targeting these mechanisms are beginning to be uncovered as well.[14,15]

The ongoing phage-bacteria arms race is highlighted by instances where defense systems detect interference by specific anti-defense genes. For example, systems like retrons,[16,17] Ronin, and phage anti-restriction-induced system (PARIS)[18,19] can sense tampering of other defense systems by phages and trigger additional defensive measures, prompting phages to evolve further countermeasures.[20,21]

Much like bacteria do not encode every possible defense system,[22] it is likely that phages do not carry all anti-defense genes. In phages, the number of anti-defense genes may be limited by genomic constraints, as the size of a phage genome is restricted by the capacity of the capsid.[23] In addition, some anti-defense proteins such as overcome classical restriction (Ocr) are sensed by specific defense systems, presenting additional vulnerabilities.[18] To balance these trade-offs, it is plausible that phages carry only a subset of anti-defense genes, acquiring others through recombination with related phages.[24] These recombination events, driven by high evolutionary pressure from phage defenses, are the main drivers of phage differentiation and variability.[25] Based on this, we hypothesized that anti-defense genes are likely encoded in regions of high genomic variability within phage genomes. To test this hypothesis, we used phages of the *Pbunavirus* genus, which infect *Pseudomonas* species[26] and have been used in pre-clinical studies and clinical trials for phage therapy, as a model.[27,28] By analyzing regions of high genomic variability in these phages, we selected 43 candidate genes and tested them for anti-defense activity against a panel of 12 individual defense systems in *Pseudomonas aeruginosa* strain PAO1. Our screen identified five anti-defense genes: one inhibiting Druantia type III, named DadIII-1; another targeting Thoeris type III, named TadIII-1; one inhibiting Zorya type I, named ZadI-1; and two related broad defense inhibitors, named Bdi1 and Bdi2 targeting four defense systems, including Zorya

type I, restriction-by-an-adenosine-deaminase-acting-on-RNA (RADAR), Hypnos, and Druantia type I. This approach demonstrates the potential for identifying anti-defense genes by exploring variable regions of phage genomes and sets the stage for broader investigations across other phage taxonomic groups. Understanding the full repertoire of phage anti-defense mechanisms will not only shed light on phage evolution but also advance the development of phage-based therapeutics.

RESULTS

Uncovering anti-defense genes in highly variable genomic regions of *Pbunavirus*

To uncover unknown anti-defense genes in highly variable regions of phage genomes, we analyzed the pangenome of 162 *Pbunavirus* genomes available in RefSeq using Partitioned PanGenome Graph Of Linked Neighbors (PPanGGOLiN).[29] This analysis categorized the genes into three distinct groups: 30 core genes (18%, present in at least 95% of genomes), 71 shell genes (39%, present in more than 1.5% and less than 95% of genomes), and 66 cloud genes (42%, present in less than 1.5% of genomes) (Table S1). Notably, the highest genomic variability was observed in the 50–65 kb region, which is predominantly composed of small hypothetical proteins (Figure 1A).

To test our hypothesis that proteins with anti-defense activity are encoded in these highly variable regions, we mapped known anti-defense genes onto the *Pbunavirus* genome. This analysis identified only the gene for the anti-restriction protein Lar[30] within these variable regions (Figure 1A; Table S1). To investigate the anti-defense activity of other genes in this region, we selected 43 representative genes from the variable regions of the *Pbunavirus* pangenome (Table S2) and tested them against a collection of 12 defense systems expressed in *P. aeruginosa* strain PAO1[31,32] (Figure 1B). These candidate anti-defense genes encode proteins ranging in size from 37 to 475 amino acids, with the majority (75%) being smaller than 150 amino acids (Figure S1A).

Each candidate anti-defense gene was expressed individually from a plasmid in host cells, which were then challenged with a *Pbunavirus* that does not encode the candidate anti-defense gene. However, some defense systems, such as Druantia type I, Hypnos, and Zorya type I, failed to protect from *Pbunavirus* phages in our collection. In these cases, we used a surrogate phage from the *Autographiviridae* family, which is vulnerable to these systems, to test the effect of the candidate anti-defense genes. The combinations of defense systems and candidate anti-defense genes for testing were based on the known infectivity of *Pbunavirus* against PAO1 expressing each defense system.[31] If a defense system protected against a phage specifically encoding the candidate anti-defense gene as well, that combination was excluded from testing (Table S2).

Our search revealed five anti-defense genes targeting various defense systems, including Zorya type I, RADAR, Hypnos, Druantia types I and III, and Thoeris type III (Figure 1C). Interestingly, the validated anti-defense proteins are significantly smaller (average size: 90 amino acids) than other proteins in the *Pbunavirus* core (average: 559 amino acids), shell (average: 319 amino acids), or cloud (average: 314 amino acids) pangenomes.

Bdi1 and Bdi2 are inhibitors of a broad range of nucleic-acid-targeting defense systems

Among our candidate genes, Bdi1 (ORF83 from phage Nemo, Genbank: KT372694.1) and Bdi2 (ORF91 from vB_PaeM_FBPa10, Genbank: ON857929.1) surprisingly demonstrated broad-spectrum inhibitory activity. Both genes counteracted multiple defense systems, including Zorya type I, RADAR, Hypnos, and Druantia type I, as shown by efficiency of plating and culture collapse assays (Figures 2A and S2A). Phage propagation assays further revealed that Bdi1 and Bdi2 are similarly effective against Zorya type I. However, Bdi1 was more effective at inhibiting Hypnos and Druantia type I than Bdi2, whereas Bdi2 was more effective against RADAR (Figure S2B). To understand the broad inhibitory activity of Bdi1 and Bdi2, we first searched for functional domains at the sequence level but found none. We then analyzed the proteins at the structural level and found that, despite sharing only 33.8% identity at amino acid level (Figure S2C), Bdi1 and Bdi2 have strong structural similarity with each other (AlphaFold 3, Dali[33] *Z* score: 12.1), suggesting a similar mechanism for defense system inhibition (Figures 2B and S2D). Multimeric predictions using AlphaFold 3 suggested that Bdi1, but not Bdi2, forms multimers, with the most confident prediction being a hexamer (Figures 2C and S2E). A structural similarity search using Foldseek with the multimeric structure did not reveal any significant structural homologs, but analysis of the monomeric structure indicated significant similarity (prob 1.00, %ident 16.2, E value 7.62e−3) to elongation factor P, specifically to its N-terminal region containing a Kyprides-Ouzounis-Woese (KOW)-like domain (Figure S2F). The KOW domain is a subclass of the Src homology-3 (SH3) domain, an ancient fold that is involved in signaling pathways through protein-protein interactions.[34] The KOW-like domain is also known to function through protein-protein interactions and to bind ribonucleoproteins.[35,36] The four defense systems inhibited by Bdi1 and Bdi2 have no shared proteins or functional domains that could serve as common targets but have been shown to, or postulated to, convey defense via targeting of nucleic acids (DNA for Hypnos[32] and Druantia type I,[12] RNA for RADAR,[37,38] and DNA and RNA for Zorya type I[39]; Figure S2G). Based on this shared feature of targeting nucleic acids, we hypothesized that Bdi1 and Bdi2 may interfere with protein-nucleic-acid interactions of these defense systems, inhibiting their activity. To investigate this hypothesis, we used AlphaFold 3 to co-fold Bdi1 (predicted with higher confidence than Bdi2; Figure S2D) with each protein of the defense systems it inhibits. However, we did not observe highly confident co-folding of Bdi1 with any of the defense system proteins (Figure S2H). Because Bdi1 is inhibiting multiple DNA- and RNA-targeting defense systems, we considered whether it would act as a nucleic acid mimic, but analysis of the electrostatic charges of the monomeric or multimeric structures did not support this possibility (Figure 2D).

To further explore the multimeric structure of Bdi1, we used Predictomes,[40] an *in silico* predictive tool that analyzes AlphaFold 3 structures to identify residue pairs that are confidently predicted to engage in protein-protein interactions (Table S3). Based on this information and amino acid conservation in Bdi1 and Bdi2 homologs (Figures 2E and S2I), we selected three amino acids in Bdi1 that may contribute to multimer formation for mutational analysis (Figures 2C and 2F). Mutating each of these amino acids (D14A, L33E, and W54A) completely

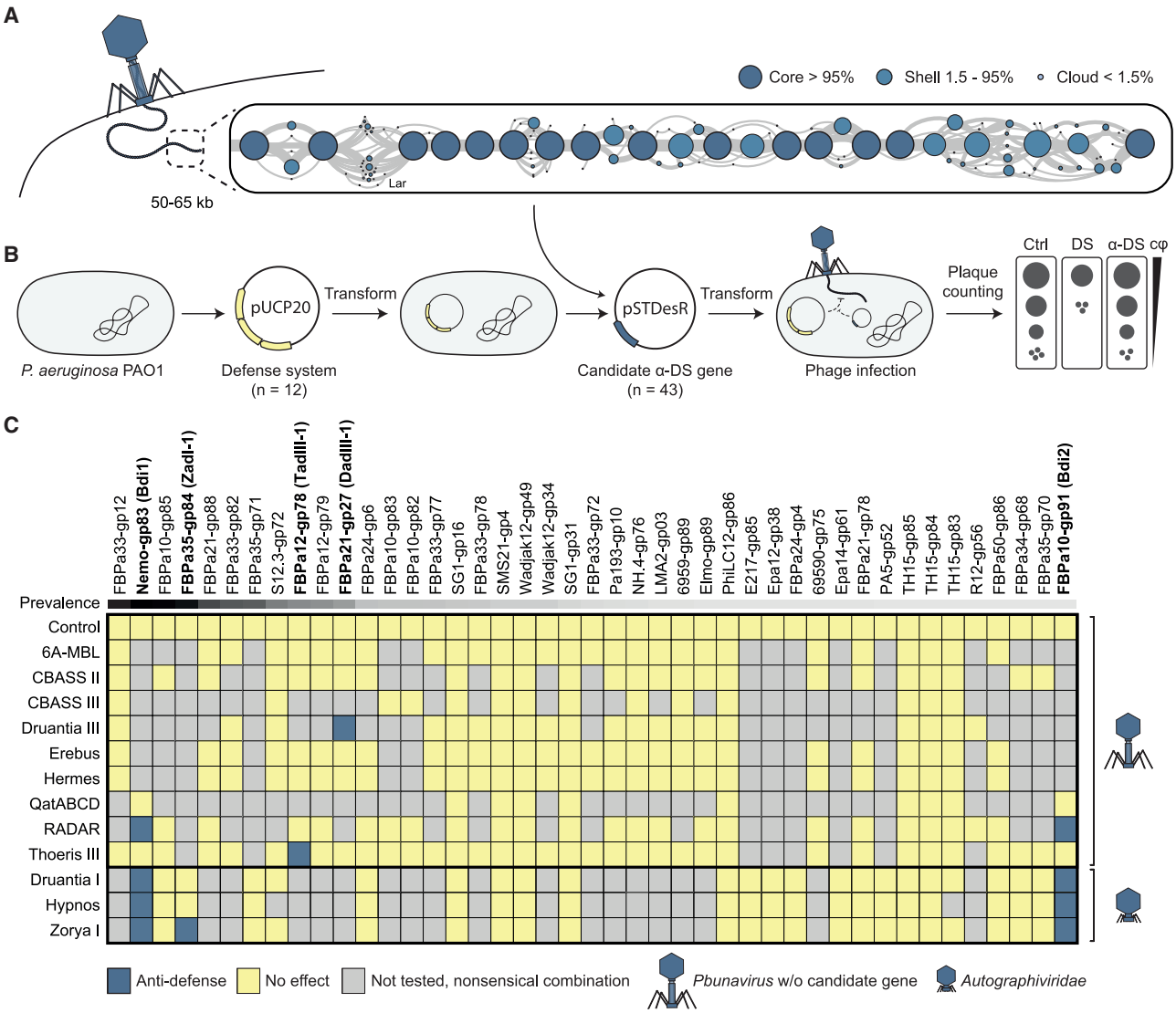

Figure 1. The pangenome of *Pbunavirus* reveals highly variable regions containing genes with anti-defense properties

(A) Representation of the pangenome of the 50–65 kb region of *Pseudomonas Pbunavirus* (*n* = 162) generated by PPanGGOLiN. Genes are classified as core when present in >95% of the genomes, as shell when found in >1.5% and <95% of the genomes, and as cloud when present in <1.5% of the genomes. The location of known anti-defense gene Lar is indicated.

(B) Individual defense systems were cloned with their native promoters into pUCP20 and then introduced into the *P. aeruginosa* strain PAO1, followed by the introduction of the candidate anti-defense gene on a second plasmid. The anti-defense activity of the candidate genes was assessed using efficiency of plating assays with a phage that does not encode the candidate anti-defense gene.

(C) Tricolor heatmap showing the combinations of defense system and candidate anti-defense gene tested. The combinations tested are shown in yellow, with those showing anti-defense properties marked in dark blue. Combinations not tested (gray) were excluded because phages carrying the candidate gene are targeted by the defense system. The anti-defense activity of the candidate gene was tested using a *Pbunavirus* where this gene is absent or tested using a podophage of the *Autographiviridae* family. The candidate genes are organized from most (left, 87%) to least (right, 0.62%) prevalent in *Pbunavirus*.

abolished the inhibitory activity of Bdi1 against Zorya type I (Figure 2F). However, none of these mutations affected the anti-defense activity of Bdi1 against RADAR, and only D14A and L33A abolished its activity against Hypnos and Druantia type I (Figure 2F). The selective effect of these mutations on each defense system suggests that Bdi1 employs distinct mechanisms to inhibit different phage defense systems, although further structural and biochemical analyses will be needed to clarify their precise mechanism of action. In summary, Bdi1 and Bdi2 function as multipurpose anti-defense proteins capable of inhibiting four defense systems involved in nucleic-acid-binding activities through a currently unknown mechanism.

ZadI-1 is an inhibitor of Zorya type I

Our search uncovered a specifically acting anti-defense gene, ZadI-1 (ORF84 of vB_PaeM_FBPa35, Genbank: ON857938.1), that partially inhibits Zorya type I defense, as shown by efficiency of plating, culture collapse, and phage propagation assays

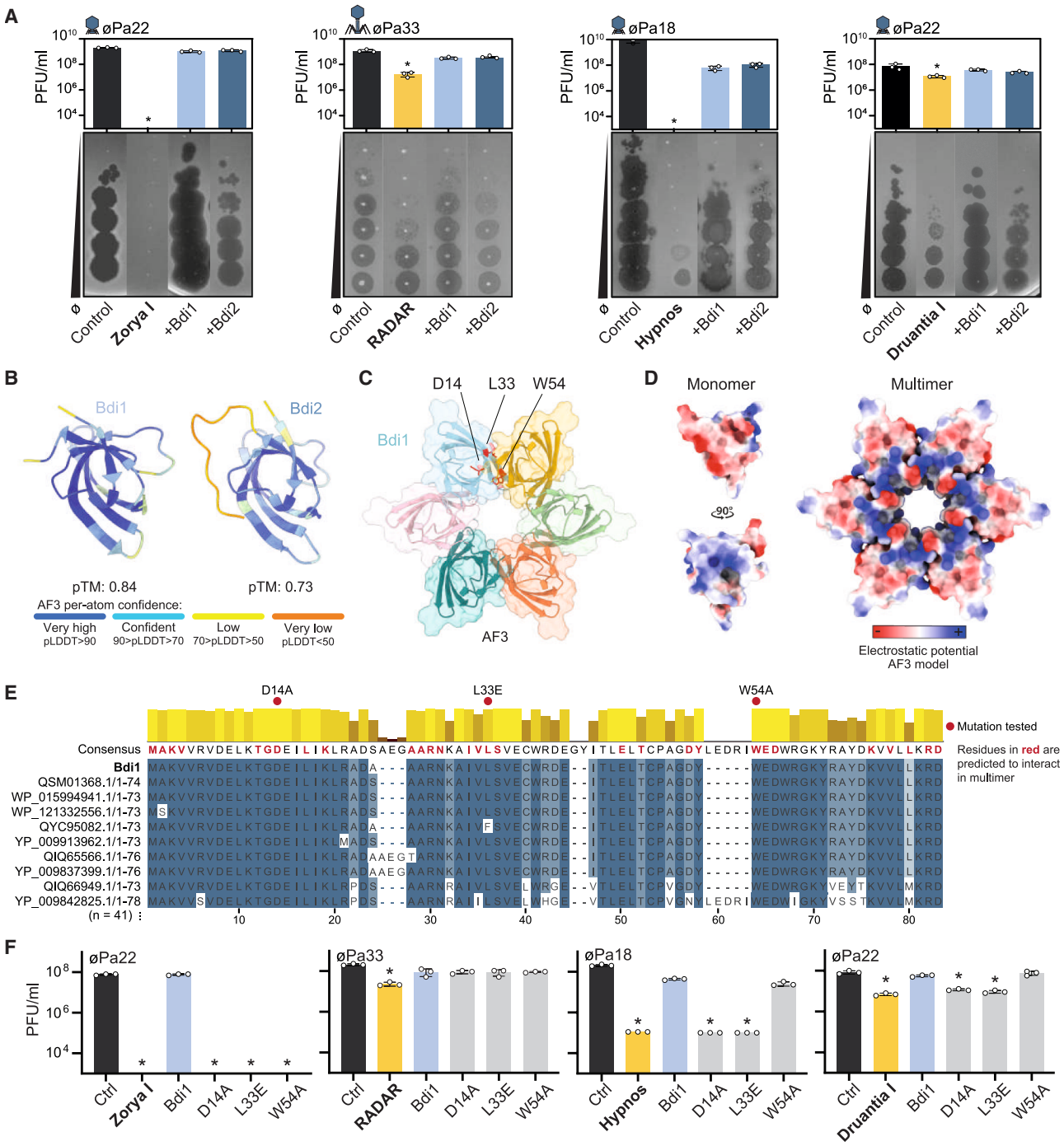

Figure 2. The inhibitory activity of Bdi1 and Bdi2 on Zorya type I, RADAR, Hypnos, and Druantia type I defense systems

(A) Effect of anti-defense proteins Bdi1 and Bdi2 on Zorya type I, RADAR, Hypnos, and Druantia type I protection against phage infection, evaluated by measuring phage titers (PFU/mL). Phage titers were determined, with an example plate shown alongside a bar graph representing the average titers from three independent biological replicates. Error bars indicate standard deviation, and statistically significant differences ($p < 0.05$) are marked with an asterisk (*). Control is *P. aeruginosa* strain PAO1 containing empty pUCP20 and pSTDesR plasmids.

(B) Monomeric structure of Bdi1 and Bdi2, as predicted by AlphaFold 3 (AF3) and colored by predicted local distance difference test (pLDDT).

(C) Hexameric structure of Bdi1, as predicted by AF3 and colored by monomer. Three amino acids of Bdi1 predicted to be important for multimer formation, and mutated in (F), are shown in red.

(D) Monomeric (left) and hexameric (right) AF3 structures of Bdi1 colored by electrostatic potential.

(legend continued on next page)

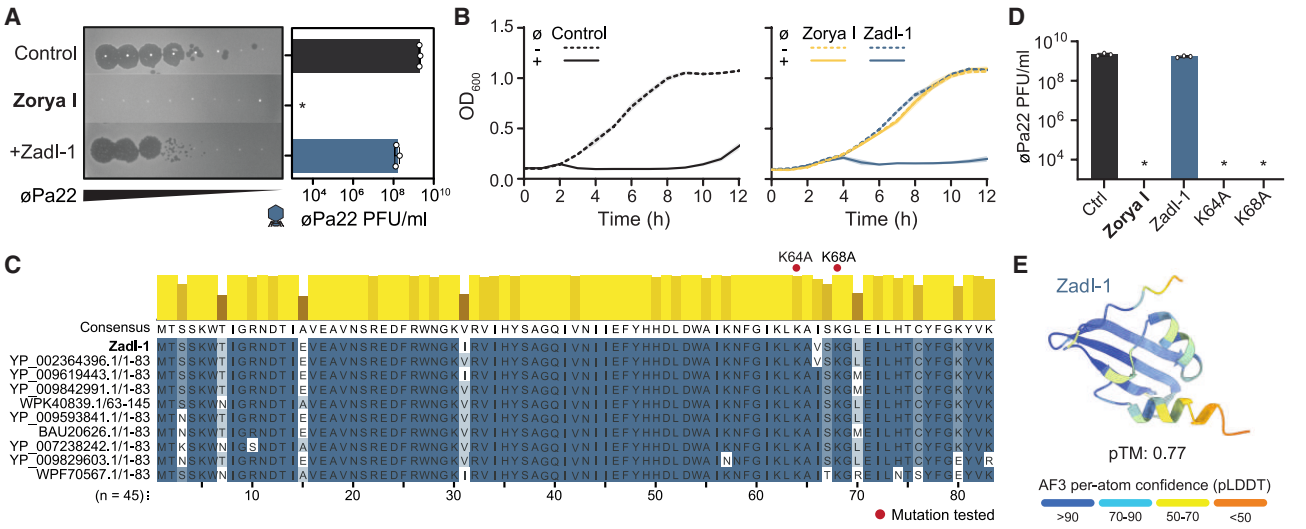

Figure 3. The inhibitory activity of ZadI-1 on ZadI-1 defense

(A) Effect of anti-defense protein ZadI-1 on Zorya type I protection against phage vB_PaeP_FBPa22 (øPa22), evaluated by measuring phage titers (PFU/mL). An example plate is shown alongside a bar graph representing the average phage titers from three independent biological replicates. Error bars indicate standard deviation, and statistically significant differences ($p < 0.05$) are marked with an asterisk (*).

(B) Effect of anti-defense protein ZadI-1 on Zorya type I protection against phage øPa22, evaluated by measuring bacterial growth via optical density (OD 600 nm). The graph displays the average OD readings and standard deviations from three biological replicates.

(C) Multiple sequence alignment of Zad-1 with 43 homologous sequences. Ten representative sequences are shown, with consensus indicated above. Mutations tested in (D) are indicated with a red dot.

(D) Effect of point mutations in selected amino acids of ZadI-1 on anti-defense activity against Zorya type I. The bar graph displays the average phage titers from three independent biological replicates. Error bars indicate standard deviation, and statistically significant differences ($p < 0.05$) are marked with an asterisk (*).

(E) Structure of ZadI-1 predicted by AlphaFold 3 (AF3) and colored by pLDDT.

(Figures 3A, 3B, and S3A). Mutagenesis of two conserved lysine residues in ZadI-1 homologs (K64A and K68A) abolished the anti-defense function of ZadI-1 against Zorya type I, suggesting that these residues are important for activity (Figures 3C and 3D). Whether these effects arise from direct involvement in defense inhibition or from altered protein stability or conformation remains to be determined.

ZadI-1 does not contain any known functional domains that could suggest its mechanism of action. To explore potential functions, we used AlphaFold 3 to predict its structure. ZadI-1 shows no sequence or structural similarity to the anti-Zorya proteins Bdi1 and Bdi2, and its failure to inhibit the other defense systems affected by Bdi1 and Bdi2 suggests it acts through a distinct inhibitory mechanism. AlphaFold 3 predictions indicate that ZadI-1 likely functions as a monomer (Figure 3E) and does not support a confident interaction with the Zorya type I proteins (Figure S3B). Thus, ZadI-1 inhibits Zorya type I through a mechanism that remains elusive but is likely distinct from that of Bdi1 and Bdi2.

TadIII-1 is an inhibitor of Thoeris type III

We identified TadIII-1 (ORF78 of vB_PaeM_FBPa12, GenBank: ON857930.1), a protein that inhibits Thoeris type III defense, as demonstrated by both efficiency of plating and culture collapse assays (Figures 4A and 4B). In these assays, TadIII-1 fully restored phage infectivity in the presence of the defense system. Despite extensive analysis, we found no known functional domains in TadIII-1 or any significant structural similarity to previously characterized proteins (Figure 4C).

To identify potential interactions between TadIII-1 and the Thoeris type III components, we used co-folding predictions. TadIII-1 was weakly predicted to interact with the phage-sensing Toll-interleukin receptor (TIR) proteins ThcB1 and ThcB3, as well as SLOG-domain-containing protein ThcA (Figure S4A). Because ThcB1 is predicted to form a dimer and ThcA is predicted to interact with ThcB4,[32] we also co-folded TadIII-1 with these complexes. The results showed a confident interaction between two TadIII-1 molecules and the ThcB1 dimer (interface predicted template modelling [ipTM] = 0.73, predicted template modelling [pTM] = 0.80; Figures S4B–S4D). To investigate this potential contact, we mutated the conserved TadIII-1 amino acids T47 and S49, which are predicted to interact with ThcB1 (Figure 4D; Table S3). Mutating these amino acids individually abolished TadIII-1 anti-defense activity, suggesting that these residues are functionally or structurally important for inhibiting Thoeris type III (Figure 4E).

(E) Multiple sequence alignment of Bdi1 with 40 homologous sequences. Ten representative sequences are shown, with consensus indicated above. All residues predicted to be involved in multimer formation are marked in red in the consensus sequence, and mutations tested in (F) are indicated with a red dot.

(F) Effect of point mutations in selected amino acids of Bdi1 on anti-defense activity against Zorya type I, RADAR, Hypnos, and Druantia type I. The bar graph displays the average phage titers from three independent biological replicates. Error bars indicate standard deviation, and statistically significant differences ($p < 0.05$) are marked with an asterisk (*).

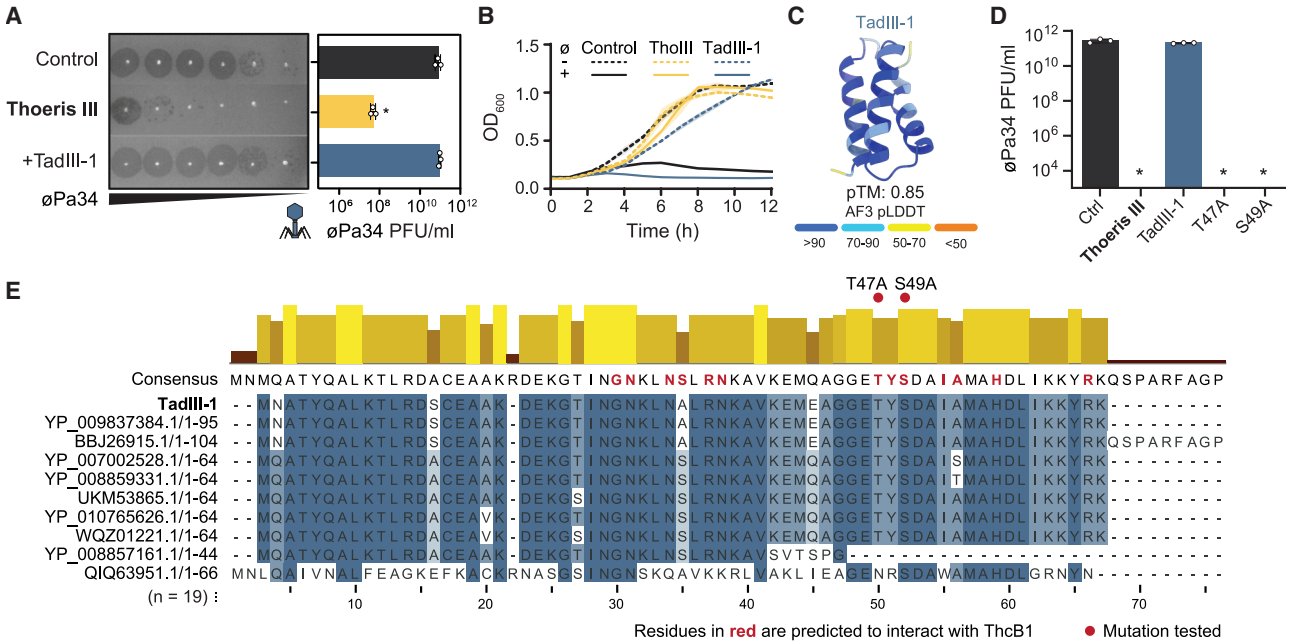

Figure 4. The inhibitory activity of TadIII-1 on Thoeris type III defense

(A) Effect of anti-defense protein TadIII-1 on Thoeris type III protection against phage vB_PaeM_FBPa34 (øPa34), evaluated by measuring phage titers (PFU/mL). An example plate is shown alongside a bar graph representing the average titers from three independent biological replicates. Error bars indicate standard deviation, and statistically significant differences ($p < 0.05$) are marked with an asterisk (*).

(B) Effect of anti-defense protein TadIII-1 on Thoeris type III protection against phage øPa34, evaluated by measuring bacterial growth via OD (600 nm). The graph displays the average readings and standard deviations from three biological replicates.

(C) Structure of TadIII-1 predicted by AF3 and colored by pLDDT.

(D) Multiple sequence alignment of TadIII-1 with 18 homologous sequences. Ten representative sequences are shown, with consensus indicated above. All residues predicted to interact with ThcB1 are marked in red in the consensus sequence, and mutations tested in (E) are indicated with a red dot.

(E) Effect of point mutations in selected amino acids of TadIII-1 on anti-defense activity against Thoeris type III. The bar graph displays the average phage titers from three independent biological replicates. Error bars indicate standard deviation, and statistically significant differences ($p < 0.05$) are marked with an asterisk (*).

To investigate the predicted interaction between TadIII-1 and ThcB1 experimentally, we performed co-purification assays with tagged versions of either TadIII-1 or ThcB1, positioning the tags at termini predicted to be minimally disruptive (Figure S4D). However, we did not detect co-purification under these conditions (Figure S4E), suggesting that if an interaction occurs, it may be weak, transient, or dependent on the native context of the Thoeris type III system. In summary, TadIII-1 inhibits the anti-phage activity of Thoeris type III by a yet unknown mechanism.

DadIII-1 is an inhibitor of Druantia type III

We identified DadIII-1 (ORF27 of vB_PaeM_FBPa21, Genbank: ON857942.1) as an anti-defense gene effective against the defense system Druantia type III, as demonstrated in efficiency of plating and culture collapse assays (Figures 5A and 5B). Druantia type III comprises the proteins DruE and DruH, with DruE being conserved across all Druantia types.[10] To determine whether DadIII-1 interferes with DruH or DruE, we tested its effect on Druantia type I, hypothesizing that if DadIII-1 targeted DruE, it would inhibit all Druantia types. We observed that DadIII-1 did not affect Druantia type I defense (Figure 5C), indicating that DadIII-1 likely targets DruH rather than DruE.

DruH lacks predicted functional domains, complicating efforts to elucidate the molecular basis for DadIII-1-mediated inhibition. Structural analysis using AlphaFold 3 did not suggest any complex formation between DadIII-1 and the Druantia type III proteins (Figures S5A and S5B), implying that inhibition may not rely on direct protein-protein interactions. However, the structural prediction of DadIII-1 was of low confidence, which limits our ability to draw conclusions about its mechanism of inhibition. This poor prediction suggests that DadIII-1 likely adopts a previously uncharacterized structure, hinting at potentially new functions. Additionally, mutating the conserved lysine residue (K85A) in DadIII-1 did not alter its anti-defense activity (Figures 5D and 5E).

In summary, the phage protein DadIII-1 inhibits Druantia type III, most likely through a mechanism specifically targeting the activity of DruH, a protein unique to this Druantia type.

Widespread occurrence of anti-defense genes in phages infecting diverse bacterial taxa

Using a sequence-based homology search, we found that several of the anti-defense genes from our study are highly prevalent in *Pbunavirus*, particularly Bdi1 (99%) and ZadI-1 (78%) (Figure 6A). These genes are often co-encoded by the same phage (Figures 6A and S6; Table S4), but we did not detect significant pairs of anti-defense genes that are significantly co-occurring, even when taking the phylogeny of the large phage terminase into account.

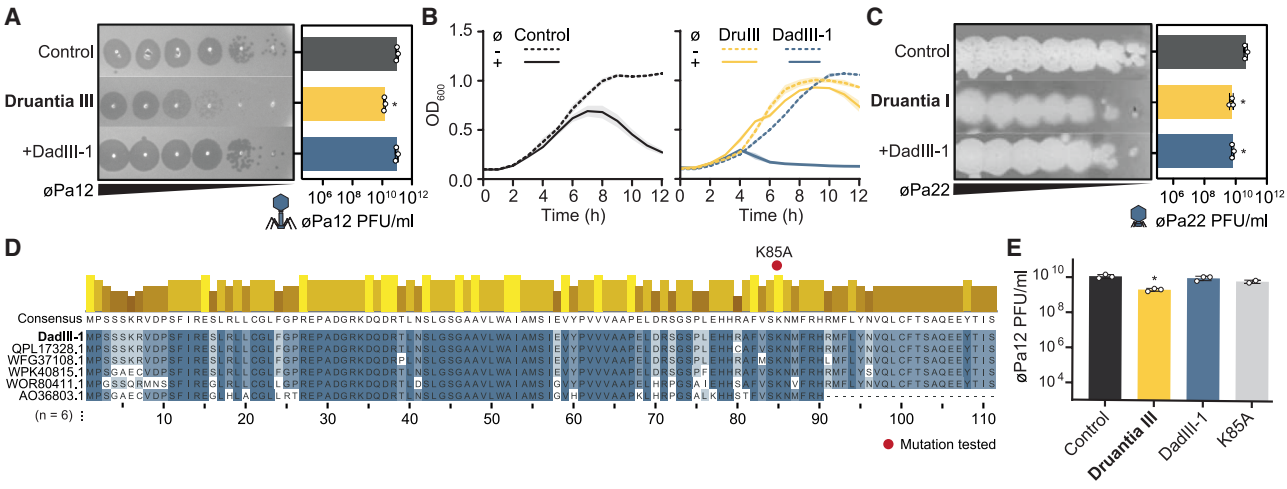

Figure 5. The inhibitory activity of DadIII-1 on Druantia type III defense

(A) Effect of anti-defense protein DadIII-1 on Druantia type III protection against phage vB_PaeM_FBPa12 (øPa12), evaluated by measuring phage titers (PFU/mL). An example plate is shown alongside a bar graph representing the average titers from three independent biological replicates. Error bars indicate standard deviation, and statistically significant differences ($p < 0.05$) are marked with an asterisk (*).

(B) Effect of anti-defense protein DadIII-1 on Druantia type III protection against phage øPa12, evaluated by measuring bacterial growth via OD (600 nm). The graph displays the average readings and standard deviations from three biological replicates.

(C) Effect of anti-defense protein DadIII-1 on Druantia type I protection against phage vB_PaeP_FBPa22 (øPa22), evaluated by measuring phage titers (PFU/mL). An example plate is shown alongside a bar graph representing the average titers from three independent biological replicates. Error bars indicate standard deviation, and statistically significant differences ($p < 0.05$) are marked with an asterisk (*).

(D) Multiple sequence alignment of DadIII-1 with its five homologous sequences. The consensus sequence is indicated on top. Mutations tested in (E) are indicated with a red dot.

(E) Effect of point mutations in a selected amino acid of DadIII-1 on anti-defense activity against Druantia type III. The bar graph displays the average phage titers from three independent biological replicates. Error bars indicate standard deviation, and statistically significant differences ($p < 0.05$) are marked with an asterisk (*).

On average, phages of the *Pbunavirus* group encode 2.9 anti-defense genes per phage (Figure 6B), but no phage encodes all six known anti-defense genes (Figures 6A and S6). This may be due to constraints such as capsid size, the metabolic burden of maintaining additional genes, or the need to balance anti-defense gene expression with evading their detection by some phage defenses. These factors suggest that the phage anti-defense pangenome acts as a reservoir from which individual phages selectively acquire anti-defense genes as needed. Supporting this, our analysis showed that anti-defense genes are unevenly distributed across different phylogenetic branches of *Pbunavirus*. For example, ZadI-1 is nearly absent in the PB1 branch, whereas Bdi2 is almost absent in the *Pseudomonas* phage Epa7, TH15, and PB1 branches (Figure 6A). These genes are typically located within clusters of small genes in highly variable regions of the phage genome (Figure S6). Interestingly, despite anti-defense activity across different phage groups (*Pbunavirus* and *Autographiviridae*), sequence similarity searches failed to detect the anti-defense genes in *Pseudomonas* phages outside the *Pbunavirus* genus, suggesting very little exchange of these genes between phage groups. The exception is ZadI-1, which was also found in the *Arenbergviridae* phage family (Figure 6C; Table S4). Furthermore, sequence similarity searches also failed to detect the anti-defense genes in phages infecting other bacterial species.

We hypothesized that the insufficient sensitivity of sequence-based approaches may limit the detection of anti-defense homologs. To overcome this, we employed a structural-based strategy, searching for structural homologs of the identified anti-defense proteins. Using AlphaFold 3 structures, we queried the Big Fantastic Virus Database (BFVD)[41] using Foldseek.[42] The BFVD consists of 351,242 viral structures, with all sequences sharing less than 30% amino acid identity. This analysis identified one structural homolog for ZadI-1 and two for TadIII-1 (Table S5). Bdi1 and Bdi2 yielded the most hits, with a total of 54 unique structural homologs distributed across more than 32 phage taxa infecting more than 17 bacteria genera. These span gram-negative and gram-positive hosts of the bacterial phyla Actinobacteria, Actinomycetota, Bacteroidota, and Pseudomonadota (Figure 6D; Table S5). Remarkably, the structural homologs of Bdi1 and Bdi2 exhibited very low sequence identity (7.4%–29.7%), highlighting the limitations of sequence-based methods for detecting these relationships (Figure 6D; Table S5).

In summary, the anti-defense genes identified in this study represent a major step in uncovering the anti-defense repertoire of phage genomes and underline the importance of phage defense systems as a barrier to phage infection. The ability of these phages to encode multiple, but not all, anti-defense genes, suggests they exploit a dynamic, largely unexplored anti-defense repertoire.

DISCUSSION

In this study, we explored the highly variable genomic regions of a common myophage infecting *P. aeruginosa* to identify anti-defense genes with either broad or specific defense inhibitory

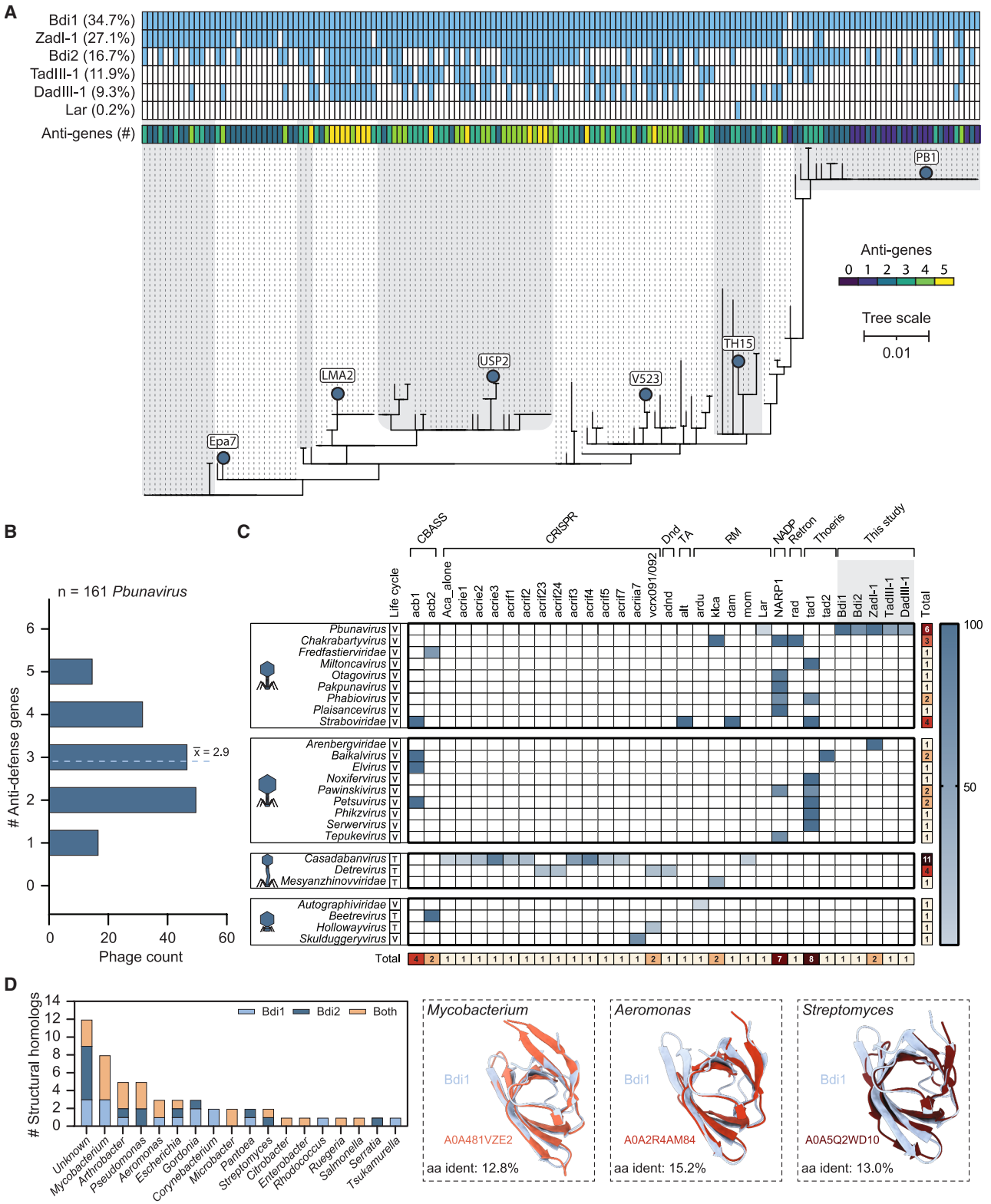

Figure 6. Distribution of anti-defense genes in *Pseudomonas* phage genomes

(A) Phylogenetic tree of *Pbunavirus*, showing the presence of anti-defense genes across the tree. Phages highlighted in Figure S6 are indicated in the tree.

(B) Prevalence of anti-defense genes across 162 *Pbunavirus* genomes. $\bar{x}$ is the average number of anti-phage defense genes per phage.

(legend continued on next page)

properties. Using *Pbunavirus* as a model phage, we identified and validated 5 out of 43 candidate genes. Collectively, these genes showed activity against 6 of the 12 defense systems tested. Among these anti-defenses, the structural homologs Bdi1 and Bdi2 individually inhibited four distinct defense systems: Zorya type I, RADAR, Hypnos, and Druantia type I. We postulate that these anti-defense genes interfere with DNA- and RNA-interacting proteins of these defense systems. Interestingly, mutational data on Bdi1 suggest distinct specificities toward different targets. Some other proteins, such as Ocr, AdrA, NARP1, and JSS1_004, have been shown to inhibit more than one phage defense system.[43–46] Ocr and AdrA achieve this by mimicking DNA and inhibiting defense systems that target specific DNA forms, whereas NARP1 overcomes NAD^+-depleting systems by reconstituting NAD^+ from its degradation products. Here, Bdi1 and Bdi2 do not seem to target conserved effector domains among defense systems, akin to JSS1_004, which inhibits several distinct defense systems via a phosphorylation-based mechanism.[46] These findings suggest that broadly acting anti-defenses are common among phages, and may provide evolutionary advantages given the genomic constraints imposed by capsid size, restricting the amount of genetic material they can encode.[47] This versatility likely arises from the functional similarities between different defense systems, which share common domains, sense similar phage-associated molecular patterns, and employ identical effector mechanisms.[48] For Bdi1 and Bdi2, it is unclear whether there is a common feature among the nucleic-acid-interacting defense systems targeted by these inhibitors and whether there are more defense systems inhibited by Bdi proteins. Given their wide distribution revealed by structural similarity searches, Bdi proteins are likely important components of the phage anti-defense repertoire in phages infecting many bacterial taxa. In addition to Bdi1 and Bdi2, we identified ZadI-1, DadIII-1, and TadIII-1 as specific inhibitors of Zorya type I, Druantia type III, and Thoeris type III defenses, respectively. Neither of these anti-defense proteins displayed structural similarity to previously characterized anti-defense proteins, highlighting the remarkable diversity of protein architectures that phages use to inhibit defense systems.

Our analysis revealed that most of the identified anti-defense genes are likely encoded on the leading strand of *Pbunavirus* genomes. This aligns with previous findings showing that anti-CRISPR proteins and other anti-defense genes also tend to be encoded on the leading strand of conjugative plasmids[49] to facilitate early expression in the host. It further predicts that the exploration of leading strands in other phage families and genera could yield further discoveries of anti-defense mechanisms.

Interestingly, although amino acid similarity searches suggest that the anti-defense genes identified in this study are restricted to *Pseudomonas* phages and largely specific to the *Pbunavirus* genus, structural analysis reveals their broader distribution across phages of multiple taxa infecting diverse bacterial hosts from all major clades. This discrepancy between sequence- and structure-similarity approaches likely arises because anti-defense genes can undergo extensive sequence divergence while retaining their structure and function, making them undetectable by sequence-based methods. In such cases, structure-based approaches can uncover relationships between genes that have diverged too far at the sequence level. These findings highlight the value of structural genomics approaches in assessing the prevalence of anti-defense genes across diverse phages, although their success ultimately depends on the accuracy of structure predictions.

Although our study shows that *Pbunavirus* typically encodes an average of three anti-defense genes, and up to five in some cases, leading to the inhibition of up to seven defense systems, anti-defense genes targeting recently discovered defense systems remain massively underrepresented.[50] It is likely that the actual number of anti-defense genes per phage, as well as the phage defense systems they inhibit, is higher than current estimates suggest. The discovery of potent, broadly acting anti-defense genes holds great potential to improve phage-based therapeutics, particularly by informing the engineering or selection of phages that can overcome abundant phage defense systems in phage-resistant pathogenic species.[31] Our study contributes valuable anti-defense genes and presents a strategy for discovering others by exploring highly variable regions in genomes of other phage groups.

Limitations of the study

Our study reveals anti-defense proteins against a variety of phage defense systems, but many open questions remain. We used structural predictions and mutational analysis to explore possible molecular mechanisms but were not able to determine how these proteins inhibit phage defense systems. For example, AlphaFold-based co-folding suggests a potential interaction between TadIII-1 and Thoeris components, but we were unable to confirm this experimentally. It is possible that the inhibition does not involve direct blocking interactions with Thoeris type III proteins, similar to other anti-Thoeris proteins that act by binding or degrading signaling molecules, but it is also possible that the interaction is too weak or transient to detect in our heterologous *E. coli* system. In addition, the interaction might depend on the presence of the other Thoeris type III components or factors only present during phage infection in *P. aeruginosa*. Further studies will be required to elucidate the mechanisms of inhibition.

RESOURCE AVAILABILITY

Lead contact

Requests for further information, resources, and data should be directed to, and will be fulfilled by, the lead contact, Stan J.J. Brouns (stanbrouns@gmail.com).

(C) Distribution of anti-defense genes across different phage taxonomic groups infecting *Pseudomonas*, with their life cycle denoted by a "V" for virulent and a "T" for temperate phages.

(D) Diversity of host genera of phages encoding Bdi1 and Bdi2 structural homologs found in the Big Fantastic Virus Database (BFVD),[41] a database of 351,242 viral structures sharing less than 30% amino acid identity. The structural alignment of Bdi1 with example homologs is depicted on the right, with the amino acid identity indicated at the bottom.

Materials availability

All unique bacterial strains, phages, and plasmids generated in this study are available from the lead contact without restriction.

Data and code availability

- Phylogenetic tree, multiple sequence alignments, protein HMM profiles, Foldseek 3Di sequence, and raw liquid culture data have been deposited at Zenodo at https://doi.org/10.5281/zenodo.15603893 and are publicly available as of the date of publication.
- All original code has been deposited at Zenodo at https://doi.org/10.5281/zenodo.15603893 and is publicly available as of the date of publication.
- Any additional information required to reanalyze the data reported in this paper is available from the lead contact upon request.

ACKNOWLEDGMENTS

This work was supported by grants from the European Research Council (ERC) CoG under the European Union's Horizon 2020 research and innovation program (grant agreement no. 101003229). N.P. is supported by the NWO NACTAR program (no. 20794). K.K. is supported by a Novo Nordisk Foundation Young Investigator Award (grant no. NNF16OC0020670) and a postdoctoral fellowship grant from the Independent Research Fund Denmark (grant no. 4257-00010B). We thank Professor Rob Lavigne from KU Leuven for kindly providing plasmid pSTDesR and Dr. Nicholas M.I. Taylor and Dr. Haidai Hu from the University of Copenhagen for providing plasmid pET11a. We are grateful to the DTU Proteomics Core Facility for maintenance and running of MS instruments. We also thank members of the Brouns lab for the many discussions and ideas that improved our work.

AUTHOR CONTRIBUTIONS

Conceptualization, S.J.J.B.; methodology, A.R.C., D.F.v.d.B., J.Q.E., H.v.d.B., N.P., and K.K.; formal analysis, A.R.C., D.F.v.d.B., J.Q.E., H.v.d.B., N.P., and K.K.; investigation, A.R.C., D.F.v.d.B., J.Q.E., H.v.d.B., and N.P.; visualization, A.R.C., D.F.v.d.B., J.Q.E., H.v.d.B., and N.P.; writing – original draft, A.R.C. and D.F.v.d.B.; writing – review and editing, S.J.J.B.; resources, S.J.J.B.; and funding acquisition, S.J.J.B.

DECLARATION OF INTERESTS

The authors declare no competing interests.

STAR★METHODS

Detailed methods are provided in the online version of this paper and include the following:

- KEY RESOURCES TABLE
- EXPERIMENTAL MODEL AND STUDY PARTICIPANT DETAILS
  - Bacteria and phages
- METHOD DETAILS
  - Identification of variable genes within the pangenome of *Pbunavirus*
  - Cloning of the candidate anti-defense genes
  - Protein complex prediction
  - Selection for point mutations
  - Cloning of point mutants of the anti-defense genes
  - Efficiency of plating
  - Liquid culture collapse assays
  - Infection dynamics of phage-infected cultures
  - Co-purification assay
  - Building HMM models of the anti-defense proteins
  - Search for the anti-defense proteins in all phages
  - Structural-based homology detection
  - Comparison of the variable region of *Pbunavirus* genomes
- QUANTIFICATION AND STATISTICAL ANALYSIS

SUPPLEMENTAL INFORMATION

Supplemental information can be found online at https://doi.org/10.1016/j.chom.2025.06.010.

Received: December 15, 2024
Revised: May 12, 2025
Accepted: June 6, 2025
Published: July 9, 2025

REFERENCES

1. Piel, D., Bruto, M., Labreuche, Y., Blanquart, F., Goudenège, D., Barcia-Cruz, R., Chenivesse, S., Le Panse, S., James, A., Dubert, J., et al. (2022). Phage–host coevolution in natural populations. Nat. Microbiol. *7*, 1075–1086. https://doi.org/10.1038/s41564-022-01157-1.
2. Georjon, H., and Bernheim, A. (2023). The highly diverse antiphage defence systems of bacteria. Nat. Rev. Microbiol. *21*, 686–700. https://doi.org/10.1038/s41579-023-00934-x.
3. Hussain, F.A., Dubert, J., Elsherbini, J., Murphy, M., VanInsberghe, D., Arevalo, P., Kauffman, K., Rodino-Janeiro, B.K., Gavin, H., Gomez, A., et al. (2021). Rapid evolutionary turnover of mobile genetic elements drives bacterial resistance to phages. Science *374*, 488–492. https://doi.org/10.1126/science.abb1083.
4. Stokar-Avihail, A., Fedorenko, T., Hör, J., Garb, J., Leavitt, A., Millman, A., Shulman, G., Wojtania, N., Melamed, S., Amitai, G., et al. (2023). Discovery of phage determinants that confer sensitivity to bacterial immune systems. Cell *186*, 1863–1876.e16. https://doi.org/10.1016/j.cell.2023.02.029.
5. Hampton, H.G., Watson, B.N.J., and Fineran, P.C. (2020). The arms race between bacteria and their phage foes. Nature *577*, 327–336. https://doi.org/10.1038/s41586-019-1894-8.
6. Bondy-Denomy, J., Pawluk, A., Maxwell, K.L., and Davidson, A.R. (2013). Bacteriophage genes that inactivate the CRISPR/Cas bacterial immune system. Nature *493*, 429–432. https://doi.org/10.1038/nature11723.
7. Li, Y., and Bondy-Denomy, J. (2021). Anti-CRISPRs go viral: The infection biology of CRISPR-Cas inhibitors. Cell Host Microbe *29*, 704–714. https://doi.org/10.1016/j.chom.2020.12.007.
8. Tock, M.R., and Dryden, D.T.F. (2005). The biology of restriction and anti-restriction. Curr. Opin. Microbiol. *8*, 466–472. https://doi.org/10.1016/j.mib.2005.06.003.
9. Millman, A., Melamed, S., Leavitt, A., Doron, S., Bernheim, A., Hör, J., Garb, J., Bechon, N., Brandis, A., Lopatina, A., et al. (2022). An expanded arsenal of immune systems that protect bacteria from phages. Cell Host Microbe *30*, 1556–1569.e5. https://doi.org/10.1016/j.chom.2022.09.017.
10. Doron, S., Melamed, S., Ofir, G., Leavitt, A., Lopatina, A., Keren, M., Amitai, G., and Sorek, R. (2018). Systematic discovery of antiphage defense systems in the microbial pangenome. Science *359*, eaar4120. https://doi.org/10.1126/science.aar4120.
11. Vassallo, C.N., Doering, C.R., Littlehale, M.L., Teodoro, G.I.C., and Laub, M.T. (2022). A functional selection reveals previously undetected anti-phage defence systems in the E. coli pangenome. Nat. Microbiol. *7*, 1568–1579. https://doi.org/10.1038/s41564-022-01219-4.
12. Gao, L., Altae-Tran, H., Böhning, F., Makarova, K.S., Segel, M., Schmid-Burgk, J.L., Koob, J., Wolf, Y.I., Koonin, E.V., and Zhang, F. (2020). Diverse enzymatic activities mediate antiviral immunity in prokaryotes. Science *369*, 1077–1084. https://doi.org/10.1126/science.aba0372.
13. Mayo-Muñoz, D., Pinilla-Redondo, R., Birkholz, N., and Fineran, P.C. (2023). A host of armor: Prokaryotic immune strategies against mobile genetic elements. Cell Rep. *42*, 112672. https://doi.org/10.1016/j.celrep.2023.112672.
14. Murtazalieva, K., Mu, A., Petrovskaya, A., and Finn, R.D. (2024). The growing repertoire of phage anti-defence systems. Trends Microbiol. *32*, 1212–1228. https://doi.org/10.1016/j.tim.2024.05.005.
15. Mayo-Muñoz, D., Pinilla-Redondo, R., Camara-Wilpert, S., Birkholz, N., and Fineran, P.C. (2024). Inhibitors of bacterial immune systems: discovery,

mechanisms and applications. Nat. Rev. Genet. *25*, 237–254. https://doi.org/10.1038/s41576-023-00676-9.

16. Millman, A., Bernheim, A., Stokar-Avihail, A., Fedorenko, T., Voichek, M., Leavitt, A., Oppenheimer-Shaanan, Y., and Sorek, R. (2020). Bacterial Retrons Function In Anti-Phage Defense. Cell *183*, 1551–1561.e12. https://doi.org/10.1016/j.cell.2020.09.065.
17. Bobonis, J., Mitosch, K., Mateus, A., Karcher, N., Kritikos, G., Selkrig, J., Zietek, M., Monzon, V., Pfalz, B., Garcia-Santamarina, S., et al. (2022). Bacterial retrons encode phage-defending tripartite toxin–antitoxin systems. Nature *609*, 144–150. https://doi.org/10.1038/s41586-022-05091-4.
18. Rousset, F., Depardieu, F., Miele, S., Dowding, J., Laval, A.-L., Lieberman, E., Garry, D., Rocha, E.P.C., Bernheim, A., and Bikard, D. (2022). Phages and their satellites encode hotspots of antiviral systems. Cell Host Microbe *30*, 740–753.e5. https://doi.org/10.1016/j.chom.2022.02.018.
19. Silas, S., Carion, H., Makarova, K.S., Laderman, E., Godinez, D.S., Johnson, M., Fossati, A., Swaney, D., Bocek, M., Koonin, E.V., et al. (2023). Activation of programmed cell death and counter-defense functions of phage accessory genes. Preprint at bioRxiv. https://doi.org/10.1101/2023.04.06.535777.
20. van den Berg, D.F., van der Steen, B.A., Costa, A.R., and Brouns, S.J.J. (2023). Phage tRNAs evade tRNA-targeting host defenses through anticodon loop mutations. eLife *12*, e85183. https://doi.org/10.7554/eLife.85183.
21. Burman, N., Belukhina, S., Depardieu, F., Wilkinson, R.A., Skutel, M., Santiago-Frangos, A., Graham, A.B., Livenskyi, A., Chechenina, A., Morozova, N., et al. (2024). A virally-encoded tRNA neutralizes the PARIS antiviral defence system. Nature *634*, 424–431. https://doi.org/10.1038/s41586-024-07874-3.
22. Bernheim, A., and Sorek, R. (2020). The pan-immune system of bacteria: antiviral defence as a community resource. Nat. Rev. Microbiol. *18*, 113–119. https://doi.org/10.1038/s41579-019-0278-2.
23. Srikant, S., Guegler, C.K., and Laub, M.T. (2022). The evolution of a counter-defense mechanism in a virus constrains its host range. eLife *11*, e79549. https://doi.org/10.7554/eLife.79549.
24. Mahler, M., Costa, A.R., van Beljouw, S.P.B., Fineran, P.C., and Brouns, S.J.J. (2023). Approaches for bacteriophage genome engineering. Trends Biotechnol. *41*, 669–685. https://doi.org/10.1016/j.tibtech.2022.08.008.
25. Kupczok, A., Neve, H., Huang, K.D., Hoeppner, M.P., Heller, K.J., Franz, C.M.A.P., and Dagan, T. (2018). Rates of Mutation and Recombination in Siphoviridae Phage Genome Evolution over Three Decades. Mol. Biol. Evol. *35*, 1147–1159. https://doi.org/10.1093/molbev/msy027.
26. Ceyssens, P.-J., Noben, J.-P., Ackermann, H.-W., Verhaegen, J., De Vos, D., Pirnay, J.-P., Merabishvili, M., Vaneechoutte, M., Chibeu, A., Volckaert, G., et al. (2009). Survey of Pseudomonas aeruginosa and its phages: de novo peptide sequencing as a novel tool to assess the diversity of worldwide collected viruses. Environ. Microbiol. *11*, 1303–1313. https://doi.org/10.1111/j.1462-2920.2008.01862.x.
27. Castledine, M., Padfield, D., Sierocinski, P., Soria Pascual, J., Hughes, A., Mäkinen, L., Friman, V.-P., Pirnay, J.-P., Merabishvili, M., de Vos, D., et al. (2022). Parallel evolution of Pseudomonas aeruginosa phage resistance and virulence loss in response to phage treatment in vivo and in vitro. eLife *11*, e73679. https://doi.org/10.7554/eLife.73679.
28. Ashworth, E.A., Wright, R.C.T., Shears, R.K., Wong, J.K.L., Hassan, A., Hall, J.P.J., Kadioglu, A., and Fothergill, J.L. (2024). Exploiting lung adaptation and phage steering to clear pan-resistant Pseudomonas aeruginosa infections in vivo. Nat. Commun. *15*, 1547. https://doi.org/10.1038/s41467-024-45785-z.
29. Gautreau, G., Bazin, A., Gachet, M., Planel, R., Burlot, L., Dubois, M., Perrin, A., Médigue, C., Calteau, A., Cruveiller, S., et al. (2020). PPanGGOLiN: Depicting microbial diversity via a partitioned pangenome graph. PLoS Comput. Biol. *16*, e1007732. https://doi.org/10.1371/journal.pcbi.1007732.
30. King, G., and Murray, N.E. (1995). Restriction alleviation and modification enhancement by the Rac prophage of Escherichia coli K-12. Mol. Microbiol. *16*, 769–777. https://doi.org/10.1111/j.1365-2958.1995.tb02438.x.
31. Costa, A.R., van den Berg, D.F., Esser, J.Q., Muralidharan, A., van den Bossche, H., Bonilla, B.E., van der Steen, B.A., Haagsma, A.C., Fluit, A.C., Nobrega, F.L., et al. (2024). Accumulation of defense systems in phage-resistant strains of Pseudomonas aeruginosa. Sci. Adv. *10*, eadj0341. https://doi.org/10.1126/sciadv.adj0341.
32. van den Berg, D.F., Costa, A.R., Esser, J.Q., Stanciu, I., Geissler, J.Q., Zoumaro-Djayoon, A.D., Haas, P.-J., and Brouns, S.J.J. (2024). Bacterial homologs of innate eukaryotic antiviral defenses with anti-phage activity highlight shared evolutionary roots of viral defenses. Cell Host Microbe *32*, 1427–1443.e8. https://doi.org/10.1016/j.chom.2024.07.007.
33. Holm, L., and Laakso, L.M. (2016). Dali server update. Nucleic Acids Res. *44*, W351–W355. https://doi.org/10.1093/nar/gkw357.
34. Kurochkina, N., and Guha, U. (2013). SH3 domains: modules of protein–protein interactions. Biophys. Rev. *5*, 29–39. https://doi.org/10.1007/s12551-012-0081-z.
35. Falk, S., Tants, J.-N., Basquin, J., Thoms, M., Hurt, E., Sattler, M., and Conti, E. (2017). Structural insights into the interaction of the nuclear exosome helicase Mtr4 with the preribosomal protein Nop53. RNA *23*, 1780–1787. https://doi.org/10.1261/rna.062901.117.
36. Zuber, P.K., Hahn, L., Reinl, A., Schweimer, K., Knauer, S.H., Gottesman, M.E., Rösch, P., and Wöhrl, B.M. (2018). Structure and nucleic acid binding properties of KOW domains 4 and 6–7 of human transcription elongation factor DSIF. Sci. Rep. *8*, 11660. https://doi.org/10.1038/s41598-018-30042-3.
37. Gao, Y., Luo, X., Li, P., Li, Z., Ye, F., Liu, S., and Gao, P. (2023). Molecular basis of RADAR anti-phage supramolecular assemblies. Cell *186*, 999–1012.e20. https://doi.org/10.1016/j.cell.2023.01.026.
38. Duncan-Lowey, B., Tal, N., Johnson, A.G., Rawson, S., Mayer, M.L., Doron, S., Millman, A., Melamed, S., Fedorenko, T., Kacen, A., et al. (2023). Cryo-EM structure of the RADAR supramolecular anti-phage defense complex. Cell *186*, 987–998.e15. https://doi.org/10.1016/j.cell.2023.01.012.
39. Hu, H., Hughes, T.C.D., Popp, P.F., Roa-Eguiara, A., Martin, F.J.O., Rutbeek, N.R., Hendriks, I.A., Payne, L.J., Yan, Y., Sousa, V.K.d., et al. (2025). Structure and mechanism of Zorya anti-phage defense system. Nature *639*, 1093–1101. https://doi.org/10.1038/s41586-024-08493-8.
40. Schmid, E.W., and Walter, J.C. (2025). Predictomes, a classifier-curated database of AlphaFold-modeled protein-protein interactions. Mol. Cell *85*, 1216–1232.e5. https://doi.org/10.1016/j.molcel.2025.01.034.
41. Kim, R.S., Levy Karin, E., Mirdita, M., Chikhi, R., and Steinegger, M. (2025). BFVD—a large repository of predicted viral protein structures. Nucleic Acids Res. *53*, D340–D347. https://doi.org/10.1093/nar/gkae1119.
42. van Kempen, M., Kim, S.S., Tumescheit, C., Mirdita, M., Lee, J., Gilchrist, C.L.M., Söding, J., and Steinegger, M. (2024). Fast and accurate protein structure search with Foldseek. Nat. Biotechnol. *42*, 243–246. https://doi.org/10.1038/s41587-023-01773-0.
43. Kudryavtseva, A.A., Cséfalvay, E., Gnuchikh, E.Y., Yanovskaya, D.D., Skutel, M.A., Isaev, A.B., Bazhenov, S.V., Utkina, A.A., and Manukhov, I.V. (2023). Broadness and specificity: ArdB, ArdA, and Ocr against various restriction-modification systems. Front. Microbiol. *14*, 1133144. https://doi.org/10.3389/fmicb.2023.1133144.
44. Isaev, A., Drobiazko, A., Sierro, N., Gordeeva, J., Yosef, I., Qimron, U., Ivanov, N.V., and Severinov, K. (2020). Phage T7 DNA mimic protein Ocr is a potent inhibitor of BREX defence. Nucleic Acids Res. *48*, 5397–5406. https://doi.org/10.1093/nar/gkaa290.
45. Osterman, I., Samra, H., Rousset, F., Loseva, E., Itkin, M., Malitsky, S., Yirmiya, E., Millman, A., and Sorek, R. (2024). Phages reconstitute NAD^+ to counter bacterial immunity. Nature *634*, 1160–1167. https://doi.org/10.1038/s41586-024-07986-w.
46. Jiang, S., Chen, C., Huang, W., He, Y., Du, X., Wang, Y., Ou, H., Deng, Z., Xu, C., Jiang, L., et al. (2024). A widespread phage-encoded kinase

enables evasion of multiple host antiphage defence systems. Nat. Microbiol. *9*, 3226–3239. https://doi.org/10.1038/s41564-024-01851-2.

47. Nurmemmedov, E., Castelnovo, M., Catalano, C.E., and Evilevitch, A. (2007). Biophysics of viral infectivity: matching genome length with capsid size. Q. Rev. Biophys. *40*, 327–356. https://doi.org/10.1017/S0033583508004666.
48. Mariano, G., and Blower, T.R. (2023). Conserved domains can be found across distinct phage defence systems. Mol. Microbiol. *120*, 45–53. https://doi.org/10.1111/mmi.15047.
49. Samuel, B., Mittelman, K., Croitoru, S.Y., Ben Haim, M., and Burstein, D. (2024). Diverse anti-defence systems are encoded in the leading region of plasmids. Nature *635*, 186–192. https://doi.org/10.1038/s41586-024-07994-w.
50. Tesson, F., Huiting, E., Wei, L., Ren, J., Johnson, M., Planel, R., Cury, J., Feng, Y., Bondy-Denomy, J., and Bernheim, A. (2025). Exploring the diversity of anti-defense systems across prokaryotes, phages and mobile genetic elements. Nucleic Acids Res. *53*, gkae1171. https://doi.org/10.1093/nar/gkae1171.
51. Abramson, J., Adler, J., Dunger, J., Evans, R., Green, T., Pritzel, A., Ronneberger, O., Willmore, L., Ballard, A.J., Bambrick, J., et al. (2024). Accurate structure prediction of biomolecular interactions with AlphaFold 3. Nature *630*, 493–500. https://doi.org/10.1038/s41586-024-07487-w.
52. Marchler-Bauer, A., and Bryant, S.H. (2004). CD-Search: protein domain annotations on the fly. Nucleic Acids Res. *32*, W327–W331. https://doi.org/10.1093/nar/gkh454.
53. Gilchrist, C.L.M., and Chooi, Y.-H. (2021). clinker & clustermap.js: automatic generation of gene cluster comparison figures. Bioinformatics *37*, 2473–2475. https://doi.org/10.1093/bioinformatics/btab007.
54. Thompson, J.D., Higgins, D.G., and Gibson, T.J. (1994). CLUSTAL W: improving the sensitivity of progressive multiple sequence alignment through sequence weighting, position-specific gap penalties and weight matrix choice. Nucleic Acids Res. *22*, 4673–4680. https://doi.org/10.1093/nar/22.22.4673.
55. Yan, Y., Zheng, J., Zhang, X., and Yin, Y. (2024). dbAPIS: a database of anti-prokaryotic immune system genes. Nucleic Acids Res. *52*, D419–D425. https://doi.org/10.1093/nar/gkad932.
56. Lees, J., Yeats, C., Perkins, J., Sillitoe, I., Rentzsch, R., Dessailly, B.H., and Orengo, C. (2012). Gene3D: a domain-based resource for comparative genomics, functional annotation and protein network analysis. Nucleic Acids Res. *40*, D465–D471. https://doi.org/10.1093/nar/gkr1181.
57. Finn, R.D., Clements, J., and Eddy, S.R. (2011). HMMER web server: interactive sequence similarity searching. Nucleic Acids Res. *39*, W29–W37. https://doi.org/10.1093/nar/gkr367.
58. Jones, P., Binns, D., Chang, H.-Y., Fraser, M., Li, W., McAnulla, C., McWilliam, H., Maslen, J., Mitchell, A., Nuka, G., et al. (2014). InterProScan 5: genome-scale protein function classification. Bioinformatics *30*, 1236–1240. https://doi.org/10.1093/bioinformatics/btu031.
59. Trifinopoulos, J., Nguyen, L.-T., von Haeseler, A., and Minh, B.Q. (2016). W-IQ-TREE: a fast online phylogenetic tool for maximum likelihood analysis. Nucleic Acids Res. *44*, W232–W235. https://doi.org/10.1093/nar/gkw256.
60. Katoh, K., Misawa, K., Kuma, K.i., and Miyata, T. (2002). MAFFT: a novel method for rapid multiple sequence alignment based on fast Fourier transform. Nucleic Acids Res. *30*, 3059–3066. https://doi.org/10.1093/nar/gkf436.
61. Steinegger, M., and Söding, J. (2017). MMseqs2 enables sensitive protein sequence searching for the analysis of massive data sets. Nat. Biotechnol. *35*, 1026–1028. https://doi.org/10.1038/nbt.3988.
62. Necci, M., Piovesan, D., Dosztányi, Z., and Tosatto, S.C.E. (2017). MobiDB-lite: fast and highly specific consensus prediction of intrinsic disorder in proteins. Bioinformatics *33*, 1402–1404. https://doi.org/10.1093/bioinformatics/btx015.
63. Mi, H., Muruganujan, A., and Thomas, P.D. (2013). PANTHER in 2013: modeling the evolution of gene function, and other gene attributes, in the context of phylogenetic trees. Nucleic Acids Res. *41*, D377–D386. https://doi.org/10.1093/nar/gks1118.
64. Käll, L., Krogh, A., and Sonnhammer, E.L.L. (2004). A Combined Transmembrane Topology and Signal Peptide Prediction Method. J. Mol. Biol. *338*, 1027–1036. https://doi.org/10.1016/j.jmb.2004.03.016.
65. Sigrist, C.J.A., de Castro, E., Cerutti, L., Cuche, B.A., Hulo, N., Bridge, A., Bougueleret, L., and Xenarios, I. (2013). New and continuing developments at PROSITE. Nucleic Acids Res. *41*, D344–D347. https://doi.org/10.1093/nar/gks1067.
66. Altschul, S.F., Madden, T.L., Schäffer, A.A., Zhang, J., Zhang, Z., Miller, W., and Lipman, D.J. (1997). Gapped BLAST and PSI-BLAST: a new generation of protein database search programs. Nucleic Acids Res. *25*, 3389–3402. https://doi.org/10.1093/nar/25.17.3389.
67. Bazin, A., Gautreau, G., Médigue, C., Vallenet, D., and Calteau, A. (2020). panRGP: a pangenome-based method to predict genomic islands and explore their diversity. Bioinformatics *36*, i651–i658. https://doi.org/10.1093/bioinformatics/btaa792.
68. Choi, K.-H., Kumar, A., and Schweizer, H.P. (2006). A 10-min method for preparation of highly electrocompetent Pseudomonas aeruginosa cells: Application for DNA fragment transfer between chromosomes and plasmid transformation. J. Microbiol. Meth. *64*, 391–397. https://doi.org/10.1016/j.mimet.2005.06.001.
69. Mazzocco, A., Waddell, T.E., Lingohr, E., and Johnson, R.P. (2009). Enumeration of Bacteriophages Using the Small Drop Plaque Assay System. In Bacteriophages: Methods and Protocols, Volume 1: Isolation, Characterization, and Interactions, M.R.J. Clokie and A.M. Kropinski, eds. (Humana Press), pp. 81–85. https://doi.org/10.1007/978-1-60327-164-6_9.
70. Lammens, E.-M., Boon, M., Grimon, D., Briers, Y., and Lavigne, R. (2022). SEVAtile: a standardised DNA assembly method optimised for Pseudomonas. Microb. Biotechnol. *15*, 370–386. https://doi.org/10.1111/1751-7915.13922.

STAR★METHODS

KEY RESOURCES TABLE

REAGENT or RESOURCE	SOURCE	IDENTIFIER
Bacterial and virus strains		
PAO1	Fagenbank	N/A
vB_PaeM_FBPa10	Fagenbank	N/A
vB_PaeM_FBPa12	Fagenbank	N/A
vB_PaeP_FBPa18	Fagenbank	N/A
vB_PaeM_FBPa21	Fagenbank	N/A
vB_PaeP_FBPa22	Fagenbank	N/A
vB_PaeM_FBPa24	Fagenbank	N/A
vB_PaeM_FBPa33	Fagenbank	N/A
vB_PaeM_FBPa34	Fagenbank	N/A
vB_PaeM_FBPa35	Fagenbank	N/A
vB_PaeM_FBPa50	Fagenbank	N/A
PP7	LGC Standards	ATCC-15692-B4
Chemicals, peptides, and recombinant proteins		
Agar	Sigma-Aldrich	Cat# 05039
Agarose	Promega Corporation	Cat# V3125
Ampicillin	Carl Roth	Cat# K029.4
Biotin	Sigma-Aldrich	Cat# N8878-25G
Carbenicillin	Fisher Scientific	Cat# BP2648-5
cOmplete™, EDTA-free Protease Inhibitor Cocktail	Sigma-Aldrich	Cat# 11873580001
Dithiothreitol	Sigma-Aldrich	Cat# 43815-5G
DpnI	New England Biolabs	Cat# R0176S
Glycerol	Fisher Scientific	Cat# 158920025
Isopropyl β-d-1-thiogalactopyranoside (IPTG)	Sigma-Aldrich	Cat# I5502
L-arabinose	Sigma-Aldrich	Cat# A3256-100
Lysogeny Broth (LB)	Sigma-Aldrich	Cat# L3022
Magnesium chloride	Fisher Scientific	Cat# AM9530G
MES SDS Running Buffer Powder	GenScript	Cat# M00677
NEB 5-alpha competent E. coli	New England Biolabs	Cat# C2987H
Phosphate buffered saline (PBS) tablets	Calbiochem	Cat# 524650-EA
Potassium chloride	Sigma-Aldrich	Cat# P3911-500G
Precision Plus Protein- Dual Xtra Prestained Protein Standards	Bio-Rad	Cat# 1610377
Q5 DNA polymerase	New England Biolabs	Cat# M0491L
Rhamnose	Fisher Scientific	Cat# 10583731
Sodium chloride	Fisher Scientific	Cat# AC424290010
Strep-Tactin XT 4Flow high-capacity resin	IBA Lifesciences	Cat# 2-5030-002
Streptomycin sulfate salt	Sigma Aldrich	Cat# S9137-25G
SurePAGE™, Bis-Tris, 10x8, 4-20%, 10 wells	GenScript	Cat# M00655
T4 DNA Ligase	New England Biolabs	Cat# M0202S
TAE 40X	Promega Corporation	Cat# V4281
Tris base	Sigma-Aldrich	Cat# 10708976001
Critical commercial assays		
GeneJET Plasmid Miniprep Kit	Fisher Scientific	Cat# K0503
NEBuilder® HiFi DNA Assembly Master Mix	New England Biolabs	Cat# E2621L
Zymoclean Gel DNA Recovery Kit	Zymo Research	Cat# D4002

(*Continued on next page*)

Continued

REAGENT or RESOURCE	SOURCE	IDENTIFIER
Deposited data		
Phylogenetic tree, multiple sequence alignments and HMM profiles of individual anti-defense proteins; code for searching structural homologs; and Foldseek 3Di sequences; raw data of liquid culture assays	This study	Zenodo: https://doi.org/10.5281/zenodo.15603893
Oligonucleotides		
All the DNA oligonucleotides are listed in Table S5	IDT	N/A
Recombinant DNA		
All plasmids are listed and described in Table S6	N/A	N/A
gBlock gene fragments are listed in Table S5	IDT	N/A
Software and algorithms		
Adobe Illustrator 26.0.1	Adobe	N/A
AlphaFold 3	Abramson et al.[51]	https://alphafoldserver.com/
Anti-DefenseFinder v1.0.0	Tesson et al.[50]	https://github.com/mdmparis/defense-finder
CD-SearchD v3.20	Marchler-Bauer and Bryant[52]	https://www.ncbi.nlm.nih.gov/Structure/cdd/wrpsb.cgi
ChimeraX	University of California, San Francisco (UCSF)	N/A
Clinker v1.33	Gilchrist and Chooi[53]	https://github.com/Oshlack/Clinker/releases
Clustal W v2.1	Thompon et al.[54]	http://www.clustal.org/clustal2/
Dali	Holm and Laakso[33]	http://ekhidna2.biocenter.helsinki.fi/dali/
dbAPIS	Yan et al.[55]	https://github.com/azureycy/dbAPIS
Foldseek v6	van Kempen et al.[42]	https://github.com/steineggerlab/foldseek
Gene3D	Lees et al.[56]	http://gene3d.biochem.ucl.ac.uk/
GraphPad Prism 7.00	GraphPad	N/A
Hmmbuild v3.4	Finn et al.[57]	https://anaconda.org/bioconda/hmmer
HMMER v3.3.2	Finn et al.[57]	https://github.com/EddyRivasLab/hmmer
hmmsearch v3.4	Finn et al.[57]	https://github.com/madscientist01/hmmsearch
InterProScan v5.60-92.0	Jones et al.[58]	https://github.com/ebi-pf-team/interproscan
iQ-Tree2 v2.3.6	Trifinopoulos et al.[59]	http://www.iqtree.org/
MAFFT v7.525	Katoh et al.[60]	https://mafft.cbrc.jp/alignment/software/source.html
MMseqs2 v15.6	Steinegger and Söding[61]	https://github.com/soedinglab/MMseqs2
MobiDB-lite v3.8.4	Necci et al.[62]	https://github.com/BioComputingUP/MobiDB-lite
PANTHER	Mi et al.[63]	https://www.pantherdb.org/
Phobius v1.01	Käll et al.[64]	https://bioweb.pasteur.fr/packages/pack@phobius@1.01
PPanGGOLiN v1.2.74	Gautreau et al.[29]	https://github.com/labgem/PPanGGOLiN
Predictomes	Schmid and Walter[40]	https://predictomes.org/tools/af3/
PROSITE	Sigrist et al.[65]	https://prosite.expasy.org/
PSI-BLAST	Altschul et al.[66]	https://blast.ncbi.nlm.nih.gov/Blast.cgi?PAGE_TYPE=BlastSearch&PROGRAM=blastp&BLAST_PROGRAMS=psiBlast
Other		
Bio-Rad Gel Doc XR+	Bio-Rad	Cat# Bio-Rad Gel Doc XR+
Epoch 2 microplate reader	Biotek Instruments	Cat# EPOCH2
Nanophotometer	Implen	Cat# NP80

EXPERIMENTAL MODEL AND STUDY PARTICIPANT DETAILS

Bacteria and phages

A set of *Pbunavirus* from the Fagenbank were used to amplify candidate anti-defense genes. Phages ϕPa18, ϕPa22, ϕPa33, and ϕPa34 were used to test the effect of the candidate genes. *Escherichia coli* strain Dh5α was used for cloning plasmid pUCP20 with individual defense systems and plasmid pSTDesR with individual candidate anti-defense genes. *P. aeruginosa* strain PAO1 was used to clone both plasmids. All bacterial strains were grown in Lysogeny Broth (LB) at 37 °C and 180 rpm, or in LB agar (LBA, 1.5 % agar (w/v)) plates at 37 °C. *E. coli* strains containing pUCP20 or pSTDesR were grown in media supplemented with 100 μg/ml of ampicillin or 50 μg/ml of streptomycin, respectively. *P. aeruginosa* strains containing both plasmids were grown in media supplemented with 200 μg/ml of carbenicillin and 25 μg/ml of streptomycin. Phages were amplified in liquid media with PAO1, centrifuged at 3,000 × *g* for 15 min, filter-sterilized (0.2 μm PES), and stored at 4 °C.

METHOD DETAILS

Identification of variable genes within the pangenome of *Pbunavirus*

We used PPanGGOLiN v1.2.74[29,67] to identify the variable genes of 162 complete *Pbunavirus* from the Refseq database on August 1, 2023. A phylogenetic tree was constructed by aligning the large terminase protein sequence using MAFFT v7.525 (default settings),[60] and inferring by maximum likelihood phylogenetics with the use of IQ-tree v2.3.6 (-B 1000 –alrt 1000 –m TEST)[59] (available at the associated Zenodo dataset). Core genes (genes present in more than 95% of the genomes) were excluded from further analyses. The variable genes were clustered based on their sequence similarity using MMseqs2[61] (default settings) and subsequently annotated (July 2024) using HMMER v3.3.2,[57] CD-SearchD v3.20,[52] InterProScan v5.60-92.0,[58] Foldseek v6,[42] Phobius v1.01,[64] MobiDB-lite v3.8.4,[62] Gene3D,[56] PANTHER,[63] and PROSITE.[65] Previously identified anti-defense genes were searched for using dbAPIS[55] and Anti-DefenseFinder v1.0.0[50] with default settings. Representative variable genes within genetic hotspots were selected and tested for their anti-defense activity (Table S2).

Cloning of the candidate anti-defense genes

The selected candidate anti-defense genes were amplified from *Pbunavirus* of the Fagenbank using primers (Integrated DNA Technologies) from Table S6 with Q5 DNA Polymerase (New England Biolabs) or synthesized as gene fragments (gblocks, IDT). Plasmid pSTDesR was amplified by PCR to insert an RBS using primers from Table S6. PCR products were run on 1% agarose gels, and bands were excised and cleaned using the Zymoclean Gell DNA Recovery Kit (Zymo Research). The defense systems were cloned into pSTDesR using the NEBuilder HiFi DNA Assembly Master Mix and transformed into chemically competent NEB® 5-alpha Competent *E. coli* following the manufacturer's instructions. Plasmids were extracted using the GeneJET Plasmid Miniprep kit and confirmed by sequencing at Macrogen. Confirmed plasmids (Table S6) were transformed into PAO1 containing individual defense systems[31] by electroporation, as previously described.[68] The recovered cells were plated on LBA plates supplemented with 200 μg/ml of carbenicillin and 25 μg/ml of streptomycin.

Protein complex prediction

Protein complex predictions were performed using AlphaFold 3[51] for confirmed anti-defense and defense system proteins. Co-folding was carried out for each heteromeric and homomeric protein combination to model potential interactions. Predicted aligned error (PAE) plots were generated for these co-folded proteins to assess the likelihood of complex formation. Low PAE values, particularly in regions of overlap between the two proteins, were interpreted as indicative of potential protein-protein interactions.

Selection for point mutations

Point mutations in the anti-defense proteins were selected using two criteria: 1) Multiple protein alignments from PSI-BLAST[66] and Clustal W v2.1[54] to identify conserved amino acids (available at the associated Zenodo dataset); and 2) AlphaFold 3 co-folding predictions, followed by Predictomes[40] analysis to identify amino acids likely involved in protein-protein interactions (Table S3).

Cloning of point mutants of the anti-defense genes

Point mutations of the anti-defense genes in pSTDesR were obtained by round-the-horn site-directed mutagenesis using phosphorylated primers (Table S6) and Q5 DNA Polymerase. PCR products were digested with DpnI (NEB), and run on 1% agarose gels. The bands of correct size were extracted and cleaned with the Zymo Gel DNA Recovery Kit. The amplified plasmids were ligated with T4 DNA ligase (NEB) at room temperature for 2 hours and transformed into chemically competent NEB 5-alpha Competent *E. coli*. Plasmids were extracted using the GeneJET Plasmid Miniprep kit and confirmed by Sanger sequencing (Macrogen). Confirmed plasmids (Table S6) were transformed into PAO1 by electroporation.

Efficiency of plating

Phage stocks were 10-fold serially diluted in LB and the dilutions were spotted onto double-layer agar plates of PAO1 with 1) empty pUCP20 and empty pSTDesR, 2) pUCP20 with a defense system and empty pSTDesR, 3) empty pUCP20 and pSTDesR with the

candidate anti-defense gene, or 4) pUCP20 with a defense system and pSTDesR with the candidate gene, following the small plaque drop assay.[69] The assays were performed using top agar (0.5% agar, w/v) supplemented with 200 μg/ml of carbenicillin and 25 μg/ml of streptomycin for plasmid maintenance, and 10 mM Rhamnose[70] for induction of expression of candidate anti-defense proteins.

Liquid culture collapse assays

Overnight bacterial cultures were diluted to an OD_{600} of approximately 0.1 in LB and transferred to 96-well plates. Phages were added at a multiplicity of infection of less than 1. The plates were then incubated at 37°C, with OD_{600} readings taken every 10 minutes over a 12-hour period using an Epoch2 microplate spectrophotometer (Biotek), with double orbital shaking.

Infection dynamics of phage-infected cultures

Overnight bacterial cultures of PAO1 strains with empty pUCP20 and pSTDesR, pUCP20 containing a defense system and empty pSTDesR, or pUCP20 containing a defense system and pSTDesR containing an anti-defense gene, were diluted to an $OD_{600} \approx 0.1$. Expression of the anti-defense gene was induced with Rhamnose at 10 mM. The bacterial cultures were then infected with phage at an MOI <1 and incubated at 37°C and 180 rpm. Samples were taken at 0h, 2h, and 4h, and centrifuged at 10,000 × *g* for 2 min. The phage-containing supernatant was serially diluted in LB and spotted onto DLA plates of PAO1 to estimate phage concentration.

Co-purification assay

For co-purification assays to test interactions between TadIII-1 and ThcB1, the proteins were cloned Strep-tagged in a modified pET11a plasmid and untagged in a modified 13S-S plasmid using Gibson assembly as described above for cloning of candidate anti-defense genes (primers and plasmids listed in Table S6). Tag placement was guided by AlphaFold3 structural models, with a C-terminal Strep-tag used for ThcB1 and an N-terminal Strep-tag for TadIII-1 to minimize potential interference with the predicted interaction interface. The assemblies were transformed into chemically competent NEB® 5-alpha Competent *E. coli* following the manufacturer's instructions. Plasmids were extracted using the GeneJET Plasmid Miniprep kit and confirmed by Sanger sequencing (Macrogen). Confirmed plasmids were then transformed into BL21-AI cells by electroporation in the following combinations: pET11a-ThcB1 with 13S-S-TadIII-1 and pET11a-TadIII-1 with 13S-S-ThcB1. The recovered cells were plated on LBA plates supplemented with 100 μg/ml ampicillin and 25 μg/ml streptomycin. For each combination, a starter culture was grown in LB medium supplemented with antibiotics at 37°C with shaking until and OD_{600} >1, and used to inoculate a 2 L culture. Cultures were grown until reaching an OD_{600} ~0.5, at which point protein expression was induced by addition of 1 mM IPTG and 0.2% (w/v) L-arabinose. Induced cultures were incubated overnight at 20°C with shaking at 150 rpm, and cells were harvested by centrifugation (16,000 rpm, 30 min, 4°C). Cell pellets were washed once with ice-cold 1x PBS, and resuspended in lysis buffer (100 mM Tris-HCl, 150 mM NaCl, 1 mM DTT, 5% glycerol, pH 7.5) supplemented with a cOmplete protease inhibitor cocktail. Cells were lysed using a French press (2 passes at 1 kbar, continuous flow system), and lysates were clarified by centrifugation (16,000 rpm, 30 min, 4°C). The supernatant was filtered (0.45 μm) and subjected to affinity purification using Strep-Tactin® XT 4Flow® high-capacity resin (IBA life sciences). Bound proteins were eluted with ice-cold elution buffer (100 mM Tris-HCl, 150 mM NaCl, 1 mM DTT, 5% glycerol, 50 mM Biotin, pH 7.5). Elution fractions were analyzed by SDS-PAGE on 4-20% gradient gels using MES running buffer and Precision Plus Protein Dual Xtra Prestained Protein Standards ladder, and gels were stained with Bio-Safe Coomassie stain.

Building HMM models of the anti-defense proteins

HMM models of the anti-defense proteins were created using the PSI-BLAST-derived clusters of the *Pbunavirus* protein sequences. MAFFT was used to align the obtained protein sequences, and hmmbuild v3.4[57] was used to build the HMM models. The HMM models were applied to all viral proteins available from NCBI using hmmsearch v3.4,[57] and scoring thresholds were set based on the bimodal distribution of the HMM-hit bitscore. The HMM bit score obtained for each anti-defense gene is as follows: Bdi1, 125; Bdi2, 135; ZadI-1, 100; TadIII-1, 135; and DadIII-1, 100. The HMM profiles of the anti-defense proteins can be found at the associated Zenodo dataset.

Search for the anti-defense proteins in all phages

The HMM models were used to search for homologues of known anti-defense proteins and those found in this study in all phage proteins from RefSeq (downloaded in September 2024). Phages containing anti-defense homologues were filtered for *Pseudomonas* phages and their taxonomy recovered from the RefSeq database (Table S4).

Structural-based homology detection

Foldseek easy-search (version 9.427df8a) was used in exhaustive search mode (–exhaustive-search 1) to identify structural homologs of the identified anti-defense genes in the BFVD,[41] which contains 351,242 viral genes. The structural matches were filtered using a tmalnscore > 0.7, qcov > 0.8 and tcov > 0.8. The code used to run the Foldseek algorithms and analyze results is available at the associated Zenodo dataset. The Foldseek 3Di sequences of the anti-defense genes identified in this study are available at the associated Zenodo dataset.

Comparison of the variable region of *Pbunavirus* genomes

Clinker v1.33[53] was used to visualize the genomic context of the anti-defense genes among phages.

QUANTIFICATION AND STATISTICAL ANALYSIS

Unless stated otherwise, data are presented as the mean of biological triplicates ± standard deviation. A Bonferroni-adjusted p-value of less than 0.05 was considered significant.